XV International Conference on Computational Plasticity. Fundamentals and Applications
COMPLAS 2019
E. Oñate, D.R.J. Owen, D. Peric, M. Chiumenti & Eduardo de Souza Neto (Eds)

REDUCED FINITE ELEMENT SQUARE TECHNIQUES (RFE^2): TOWARDS INDUSTRIAL MULTISCALE FE SOFTWARE

ORIOL LLOBERAS-VALLS[*,†], MARCELO RASCHI[*], ALFREDO E. HUESPE[†,‡] AND JAVIER OLIVER[*,†]

[*] Centre Internacional de Metodes Numerics a l'Enginyeria (CIMNE)
Campus Nord UPC, 08034 Barcelona, Spain
e-mail: olloberas@cimne.upc.edu

[†] Universitat Politècnica de Catalunya (UPC) - BarcelonaTech
Campus Nord UPC, Mòdul C-1 101, c/ Jordi Girona 1-3, 08034 Barcelona, Spain

[‡] CIMEC-UNL-CONICET
Güemes 3450, Santa Fe, Argentina

Key words: FE^2 techniques, reduced order modeling, industrial FE software

Abstract. Reduced order modeling techniques proposed by the authors are assessed for an industrial case study of a 3D reinforced composite laminate. Essentially, the main dominant strain micro-structural modes are obtained through standard reduced order modeling techniques applied over snapshots of a representative training strain space. Additionally, a reduced number of integration points is obtained by exactly integrating the main energy modes resulting from the training energy snapshots. The outcome consists of a number of dominant strain modes integrated over a remarkably reduced number of integration points which provide the support to evaluate the constitutive behavior of the micro-structural phases. Results are discussed in terms of the consistency of the multiscale analysis, tunability of the microscopic material parameters and speed up ratios comparing a high fidelity simulation and the multiscale reduced order model.

1 INTRODUCTION AND SUMMARY OF THE MODEL

In a series of papers ([1], [2]), the authors have presented a reduced order model technique aiming at speeding-up the computational cost of multiscale mechanical problems where materials are intrinsically heterogeneous.

In the same spirit, this work aims at simulating problems where the behavior of the material at the structural scale is complex and can be hardly captured by means of a phenomenological one-scale approach. This typically happens when a strong dependency of the effective material properties with the micro-parameters governing the material deformation phenomena at the lower scales is observed. In this scenario, the use of a FE^2

technique [4], sketched in Figure 1, or a similar procedure, is essential. In this context, the micro-scale analysis, solved in a Representative Volume Element (RVE) Ω_μ, is performed with the present reduced model coined as Reduced Finite Element Square Technique (RFE^2).

This model is based on a Proper Orthogonal Decomposition procedure to build a reduced basis of the primary kinematic variable at the micro-scale problem, and a reduced optimized numerical quadrature rule to account for the constitutive behaviour of the micro-scale formulation.

In the present work, we leave aside the detailed description of the methodology to give particular emphasis to the numerical assessments of the RFE^2 model for solving industrial 3D problems and evaluate the attained speed-ups. In the next sub-Section we summarize the main equations describing the reduced model and the remaining part of the paper deals with the numerical assessment.

1.1 Micro-scale Problem Formulation

Following the formulation presented in [1], here particularized for small deformations, we can formulate the microscale problem in the RVE domain Ω_μ as follows.

Given the macro-scale strain, $\boldsymbol{\varepsilon}^M$, and the spaces of admissible ($\mathcal{U}_\mu^{\mathcal{E}}$) and variational ($\mathcal{V}_\mu^{\mathcal{E}}$) micro-strain fluctuations defined by:

$$\mathcal{U}_\mu^{\mathcal{E}} = \mathcal{V}_\mu^{\mathcal{E}} := \{\tilde{\boldsymbol{\varepsilon}}_\mu \quad | \quad \tilde{\boldsymbol{\varepsilon}}_\mu \in \mathbb{E}_\mu \quad \wedge \quad \int_{\Omega_\mu} \tilde{\boldsymbol{\varepsilon}}_\mu \, d\Omega_\mu = \mathbf{0}\} \,, \tag{1}$$

where $\tilde{\boldsymbol{\varepsilon}}_\mu$ is the micro-strain fluctuations in Ω_μ and $\mathbb{E}_\mu$ is the space of compatible strains; find the micro-strain $\boldsymbol{\varepsilon}_\mu = \boldsymbol{\varepsilon}^M + \tilde{\boldsymbol{\varepsilon}}_\mu$, with $\tilde{\boldsymbol{\varepsilon}}_\mu \in \mathcal{U}_\mu^{\mathcal{E}}$, such that:

$$\int_{\Omega_\mu} \boldsymbol{\sigma}_\mu(\boldsymbol{\varepsilon}_\mu, \alpha_\mu) : \delta\tilde{\boldsymbol{\varepsilon}}_\mu \, d\Omega_\mu = 0 \,; \qquad \forall \delta\tilde{\boldsymbol{\varepsilon}}_\mu \in \mathcal{V}_\mu^{\mathcal{E}} \,, \tag{2}$$

with $\boldsymbol{\sigma}_\mu$ being the micro-stresses expressed as a function of the micro-strain and the set of internal variables α_μ whose temporal evolution has to be specified with the corresponding equations as follows

$$\dot{\alpha}_\mu = g(\boldsymbol{\varepsilon}_\mu, \dot{\boldsymbol{\varepsilon}}_\mu, \alpha_\mu) \,. \tag{3}$$

The macro-stress, computed as the average value of the micro-stress $\boldsymbol{\sigma}_\mu$, is transferred to the coarse scale.

1.1.1 Reduced Finite Element Square Model (RFE^2)

The problem (1)-(3) is solved by introducing a low-dimensional vector space whose elements are the admissible micro-strain fluctuations $\tilde{\boldsymbol{\varepsilon}}_\mu$. Identical approach is taken for the micro-strain variations. Both spaces are spanned by a basis of n_ε vectors $\boldsymbol{\Psi}_j$. This basis is computed with a Proper Orthogonal Decomposition technique from a large set of micro-strain fluctuations that are obtained as solutions of the micro-cell problem during an off-line sampling process. Details of this procedure can be found in [3].

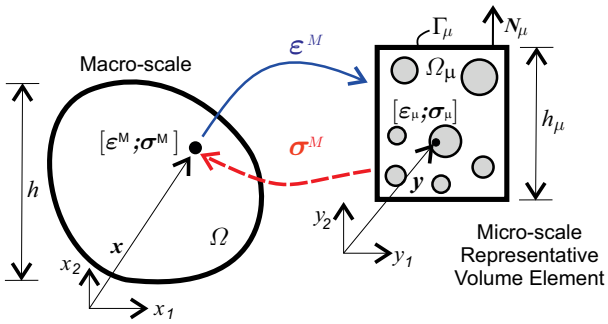

Figure 1: Structural problem involving two well-separated scales of lengths h and h_μ which satisfy $h_\mu \ll h$. Macro-scale domain is Ω and the RVE is Ω_μ. Stress and strains at Ω are denoted $\boldsymbol{\sigma}^M$ and $\boldsymbol{\varepsilon}^M$. Similar objects at the micro-scale are denoted $\boldsymbol{\sigma}_\mu$ and $\boldsymbol{\varepsilon}_\mu$. The stress $\boldsymbol{\sigma}^M$ and strain $\boldsymbol{\varepsilon}^M$ are associated with $\boldsymbol{\sigma}_\mu$ and $\boldsymbol{\varepsilon}_\mu$ through scale transitions equations.

Each element of the spaces is given by the linear combination:

$$\tilde{\boldsymbol{\varepsilon}}_\mu\left(\boldsymbol{y},t\right)=\sum_{j=1}^{n_\varepsilon}\boldsymbol{\Psi}_j\left(\boldsymbol{y}\right)c_j\left(t\right)=\boldsymbol{\Psi}(\boldsymbol{y})\boldsymbol{c}(t)\;, \tag{4}$$

where the coefficients $\boldsymbol{c}$ denote a time-dependent parameter vector. The low dimensional approach of $\tilde{\boldsymbol{\varepsilon}}_\mu$ and the corresponding variation of micro-strain fluctuation are replaced into equation (2). Furthermore, the original Gauss quadrature rule, typically used in the finite element technique to integrate the kernel of equation (2), is replaced by a reduced optimal quadrature rule with N_r reduced quadrature points[1]:

$$\int_{\Omega_\mu}(\bullet)\left(\boldsymbol{y}\right)d\Omega_\mu\approx\int_{\Omega_\mu}^{red}(\bullet)\left(\boldsymbol{y}\right)d\Omega_\mu=\sum_{k=1}^{N_r}(\bullet)\left(\boldsymbol{z}_k\right)\omega_k \tag{5}$$

The weights ω_k and spatial position $\boldsymbol{z}_k$ defining the reduced quadrature rule are defined according to the procedure described in [1].

Thus, the equation (2) can be approached as follows:

$$\int_{\Omega_\mu}\boldsymbol{\sigma}_\mu([\boldsymbol{\Psi c}],\alpha_\mu):[\boldsymbol{\Psi}\delta\boldsymbol{c}]\;d\Omega_\mu\approx\sum_{k=1}^{N_r}\left(\,\boldsymbol{\sigma}_\mu([\boldsymbol{\Psi}(\boldsymbol{z}_k)\boldsymbol{c}],\alpha_\mu(\boldsymbol{z}_k)):[\boldsymbol{\Psi}(\boldsymbol{z}_k)\delta\boldsymbol{c}]\,\right)\,\omega_k(\boldsymbol{z}_k)=\boldsymbol{0}\,;\quad\forall\delta\boldsymbol{c}\in\mathbb{R}^{n_\varepsilon}. \tag{6}$$

This system of n_ε non-linear equations is solved jointly with the evolution equations (3) evaluated in the N_r reduced quadrature points.

[1]The quadrature rule is derived from a low dimensional approach of the internal energy function ψ. A POD technique is used to extract a low dimensional basis for ψ and the reduced quadrature rule has to satisfy the correct integration of every base of ψ. This condition can be satisfied if the number of quadrature points N_r is equal to the number of modes taken for ψ plus 1. Hence, we assume that the number of modes for ψ is equal to the N_r-1.

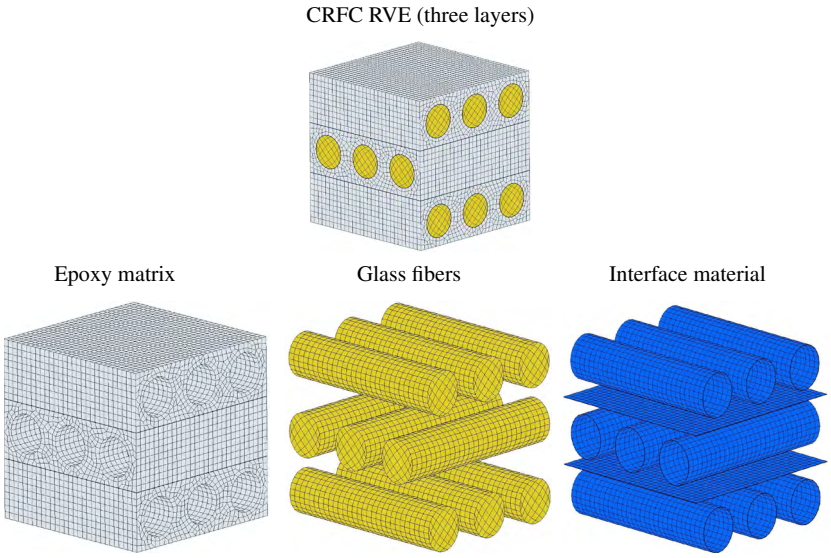

Figure 2: Material phases of the CRFC microstructural RVE.

2 RESULTS

In the following sections a number of results are commented in order to validate and demonstrate the industrial potential of the developed algorithms. The microstructure modelling is introduced and the influence of the number of strain and energy modes in the expected error is justified as well. Moreover, the RFE2 modelling is validated in terms of consistency with respect to the macro-mesh size, the number of strain modes and the corresponding number of energy modes or integration points. Tunability of the material parameters is studied as well and the obtained speed-ups for microstructures with refined discretisations is reported as well.

2.1 Microscopic modelling

The selected material is a fiber reinforced composite laminate with a microscopic representation composed by fibers (glass fiber), an epoxy matrix and an interphase material between matrix layers and fiber and matrix phases responsible for the delamination (between layers) and fiber pull-out (between fiber and matrix) effects. Fibers are assumed to behave elastically and an only-traction-damage model (cf. [5]) with hardening parameter, H, is considered with linear hardening in the matrix and interphase phases. The representation of the material phases and material parameters are given in Figure 2 and Table 1 summarizes the utilized phase parameters.

Minimal kinematic constraints (cf. equation (1)) are considered during the sampling stage of the reduction process allowing precisely to develop the observed delamination, debonding and pull-out effects. Figure 3 shows the deformed configuration and damage distribution of a sampling trajectory that involves the above mentioned physical behaviour.

After the sampling process the strain, energy bases and integration rule are retrieved

Phase	E $[N/mm^2]$	ν	Elastic limit σ_e $[N/mm^2]$	Hardening parameter H
Fiber	72000	0.25	–	–
Matrix	3790	0.37	200	10^{-1}
Interphase	3790	0.37	100	10^{-4}

Table 1: Micro material phase parameters.

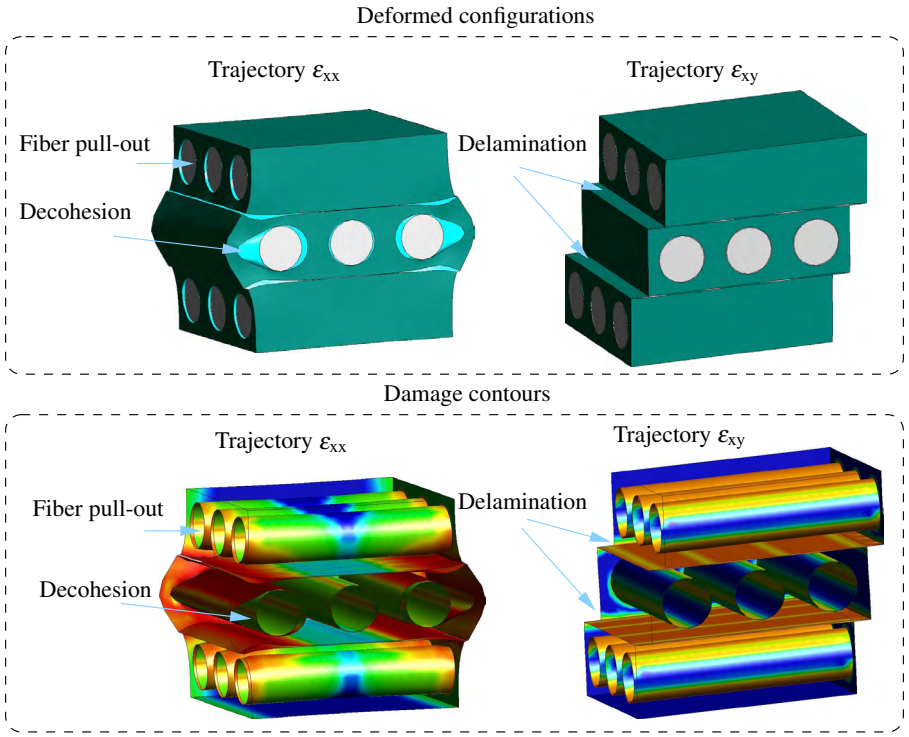

Figure 3: Deformed configuration and damage contours at trajectories ε_{xx} (left) and ε_{xy} (right).

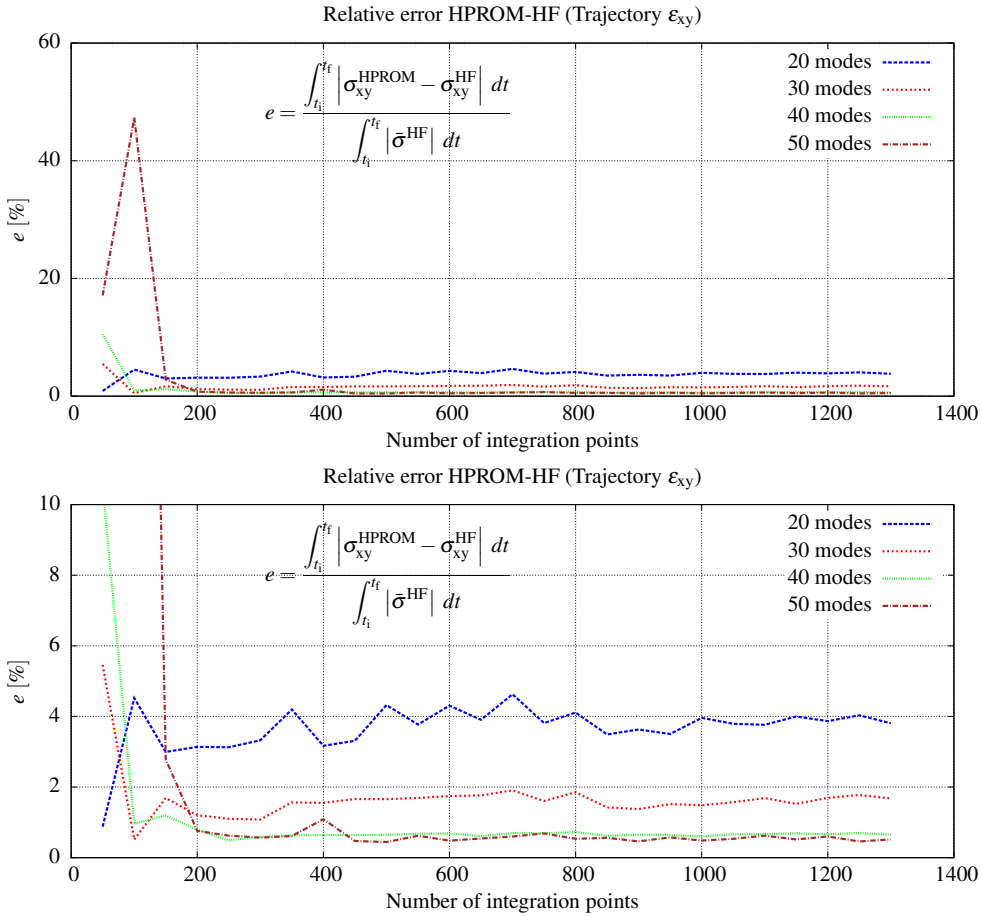

Figure 4: A posteriori error for the ε_{xy} sampling trajectory

which confers the reduced order microstructural model. The accuracy of the solution obtained with the reduced order model is compared with the high fidelity computation for a particular sampling trajectory. The obtained "a posteriori" error is plot for different reduced RVEs considering an increasing number of strain modes and integration points (cf. Figure 4). It is observed that 40 strain modes ($n_\varepsilon = 40$) and 200 integration points ($N_r = 200$) suffice to capture the physics needed to reproduce this trajectory with a relative error lower or equal than one percent.

2.2 Multiscale reduced order modelling

A dogbone specimen as depicted in Figure 5 is considered in which an imposed displacement is applied at the basis around both extremes of the specimen. The objective is to trigger, at the microstructural level, all delamination, fiber pull-out and debonding mechanisms.

A deformed configuration of the dogbone together with a displacement reconstruction

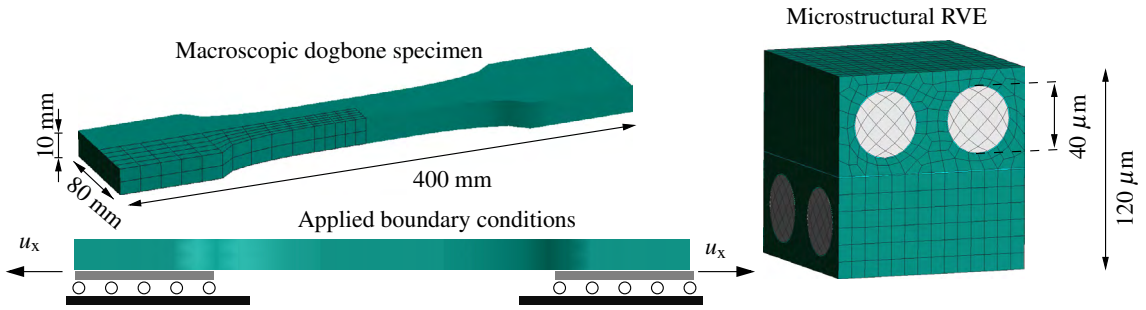

Figure 5: Multiscale analysis of a CRFC dogbone specimen under axial tension with shear: macroscopic geometry and boundary conditions (left) and microstructural RVE (right).

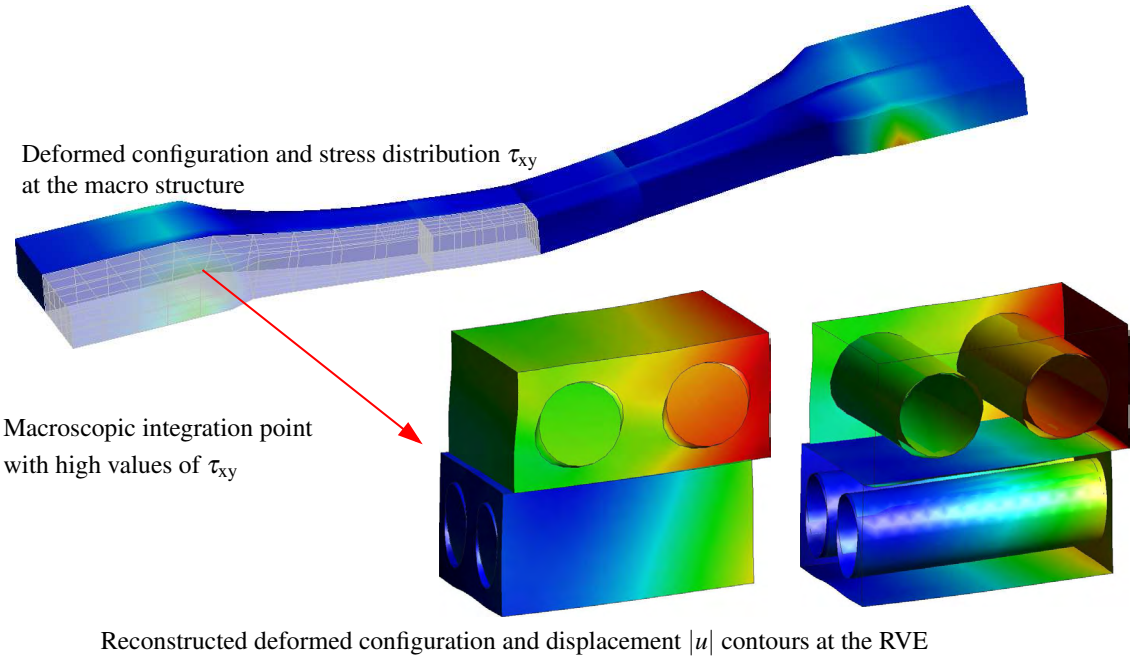

Figure 6: Deformed configuration of the macrostructure (top) and displacement reconstruction of an RVE corresponding to a critical stress point in the macro structure (bottom).

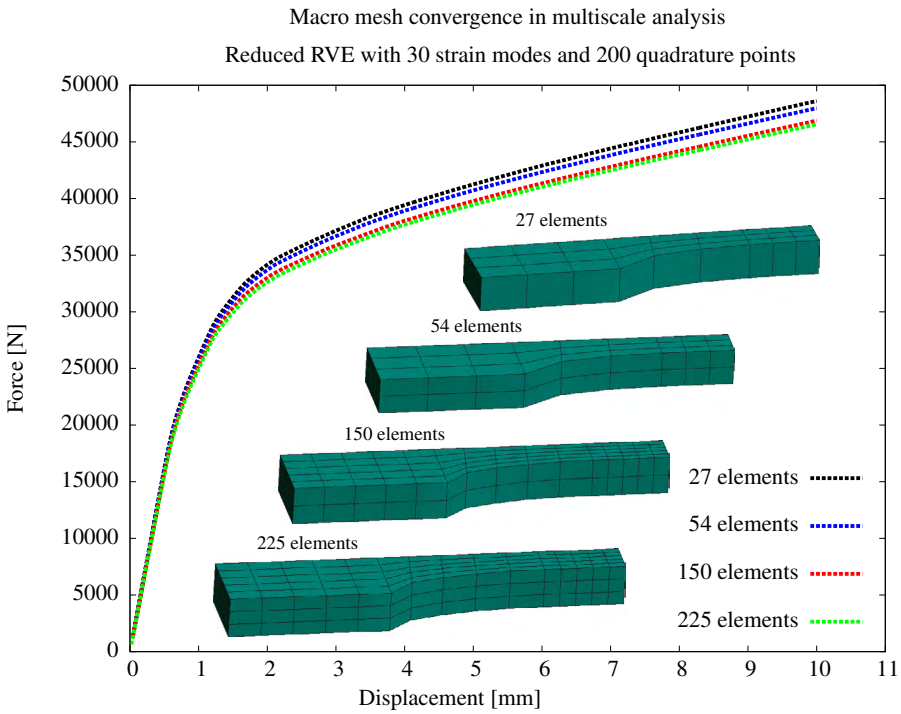

Figure 7: Global mechanical response upon mesh refinement.

of an RVE[2] corresponding to region with high σ_{xy} is given in Figure 6. The RVE reduced model accounts for 30 strain modes and 200 integration points.

2.2.1 Consistency tests

The multiscale analysis depicted in Figure 5 considering the same reduced RVE model is now repeated for a number of macroscale discretizations. The global response in terms of reaction versus applied displacement is shown in Figure 7. It is observed that the global response shows a convergent behaviour upon mesh refinement which verifies the consistency of the multiscale approach. Moreover, a sufficiently accurate response is obtained for a macroscopic discretization of around 150 elements (the total dogbone mesh being 150×4=600 elements).

Another test consists in the impact of the considered number of strain modes in the reduced RVE bases in the global response (cf. Figure 8). It turns out that 30 strain modes suffice to accurately capture the physics stemming out of the proposed multiscale problem. It is unnecessary then to consider more than 30 strain modes although a highly convergent behaviour is observed.

Finally, the number of integration points (linked to the considered energy modes) within the reduced basis is modified to study the global multiscale behaviour. To this end, the reduced RVE with 50 strain modes is considered and the number of integration points is

[2]The reconstruction stage for obtaining the micro-displacement configurations has been detailed in [1].

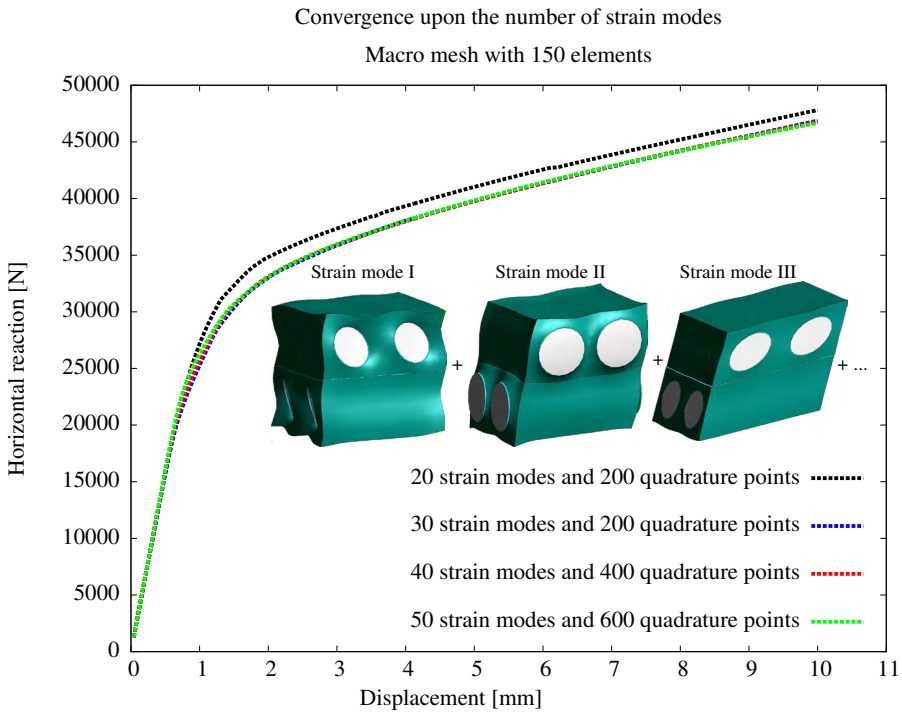

Figure 8: Global mechanical response upon increasing the micro strain modes.

increased from 200 up to 1200. Results are summarized in Figure 9 where a convergent behaviour upon increasing energy modes is observed.

2.2.2 Customization and tunability

The reduced RVE model employed in the previous sections is constructed in the bases of the material phase parameters depicted in Table 1. In order to prove the tunability of the methodology in terms of the micromaterial phase parameters a number of customization tests are outlined. First, the interphase hardening parameter and elastic limit is varied to the new values $H = 0.1$ and $\sigma_e = 175$ MPa. Figure 10 shows the resulting mechanical behaviour of the RVE obtained through a multiscale analysis and with a high fidelity analysis. The multiscale analysis is based on the RVE reduced bases obtained from a sampling procedure based on the properties depicted in Table1. If the material parameters are then modified the result is in good agreement with the response obtained from a direct FE (high fidelity) computation using such user defined parameters. Figure 11 shows a more extreme customization case in which the hardening parameter of the matrix material is set to $H = 0.9$ which is close to an elastic behaviour. It is then observed that 80 strain modes are required for the mutliscale analysis to correctly capture the desired behaviour. It is then concluded that a complete sampling renders a reduced basis capable of reproducing the mechanical behaviour upon changing the material phase parameters if enough strain modes are included in the reduced bases.

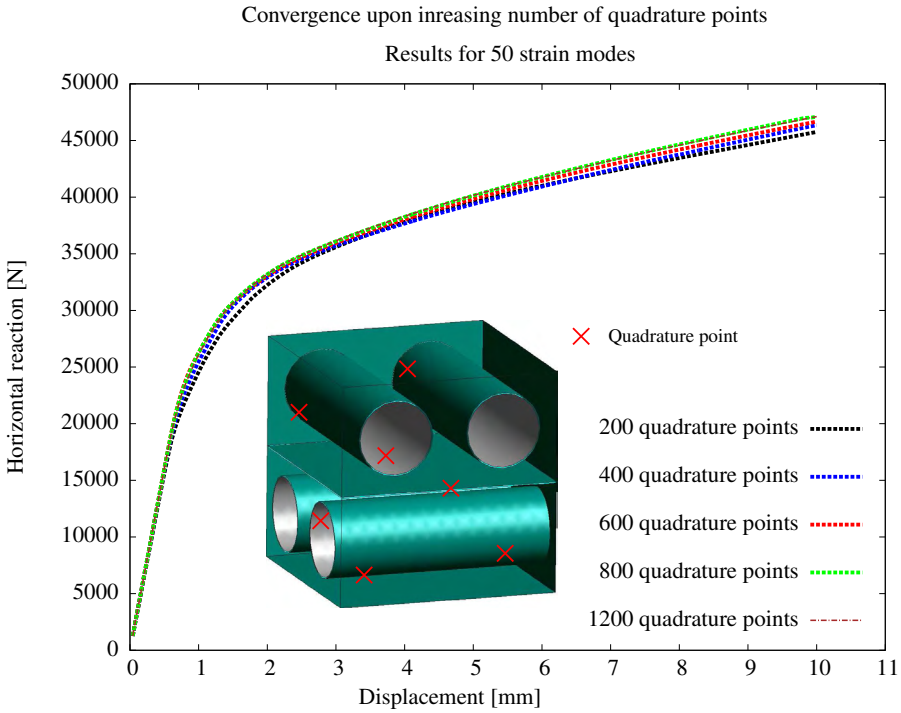

Figure 9: Global mechanical response upon increasing the micro quadrature points.

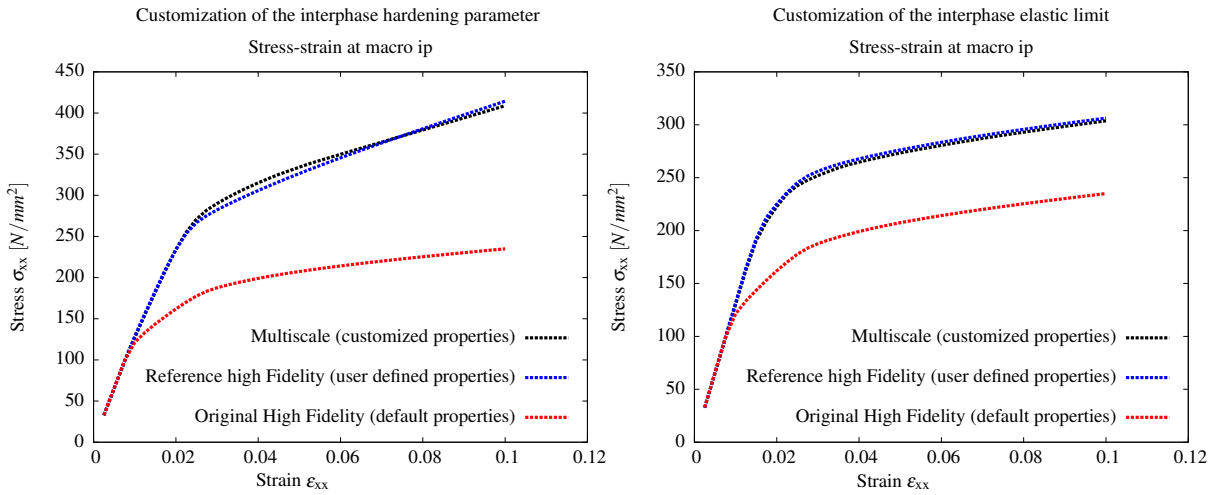

Figure 10: Tuning of the interphase hardening parameter (left) and interphase elastic limit (right). Micro-stress $(\sigma_\mu)xx$ versus micro-strain $(\varepsilon_\mu)xx$.

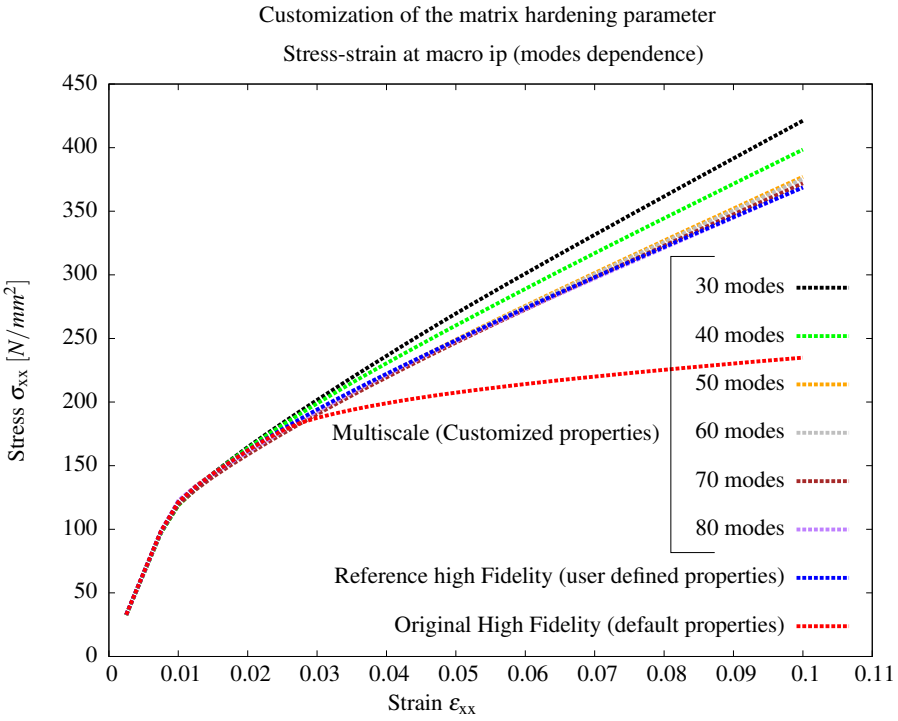

Figure 11: Tuning of the matrix hardening parameter. Micro-stress $(\sigma_\mu)xx$ versus micro-strain $(\varepsilon_\mu)xx$.

2.2.3 Computational and algorithmic Speed-up

The relative computational cost between standard FE^2 and the proposed RFE^2 technology is measured here through the algorithmic and computational speed-up, S_p. The algorithmic speed-up reflects the relative complexity of both techniques in terms of the amount of DOF to solve (DOF speed-up) and amount of quadrature points (IP speed-up). Considering that an RVE basis with 40 strain modes and 200 quadrature points suffice to provide errors below 1% when comparing the reduced order modelling and high fidelity analysis, both DOF and IP speed-ups have been calculated considering 40 DOF and 200 IP in the reduced model. Figure 12 reflects the clearly growing algorithmic speed-ups upon increasing the RVE discretization complexity. Based on the similar CRFC micro-structures with increasing number of layers and fibers one observes that for RVE discretizations with around one million of integration points the relative algorithmic speed-up is around five orders of magnitude, i.e. the reduced RVE model is expected to perform 10^4 times faster than the high fidelity one. Moreover, the reduced basis inherits the type of boundary conditions utilized during the sampling stage and, therefore, avoids any performance overhead due to handling any multi-point constraints and their impact in the bandwidth of the resulting system. Computation times have been compared regarding the high fidelity problem in one selected sampling trajectory and the reduced order model. It is seen that the resulting computational speed-up increases even more upon increasing the RVE discretization and can reach around 30×10^4 for RVEs with around one million of integration points.

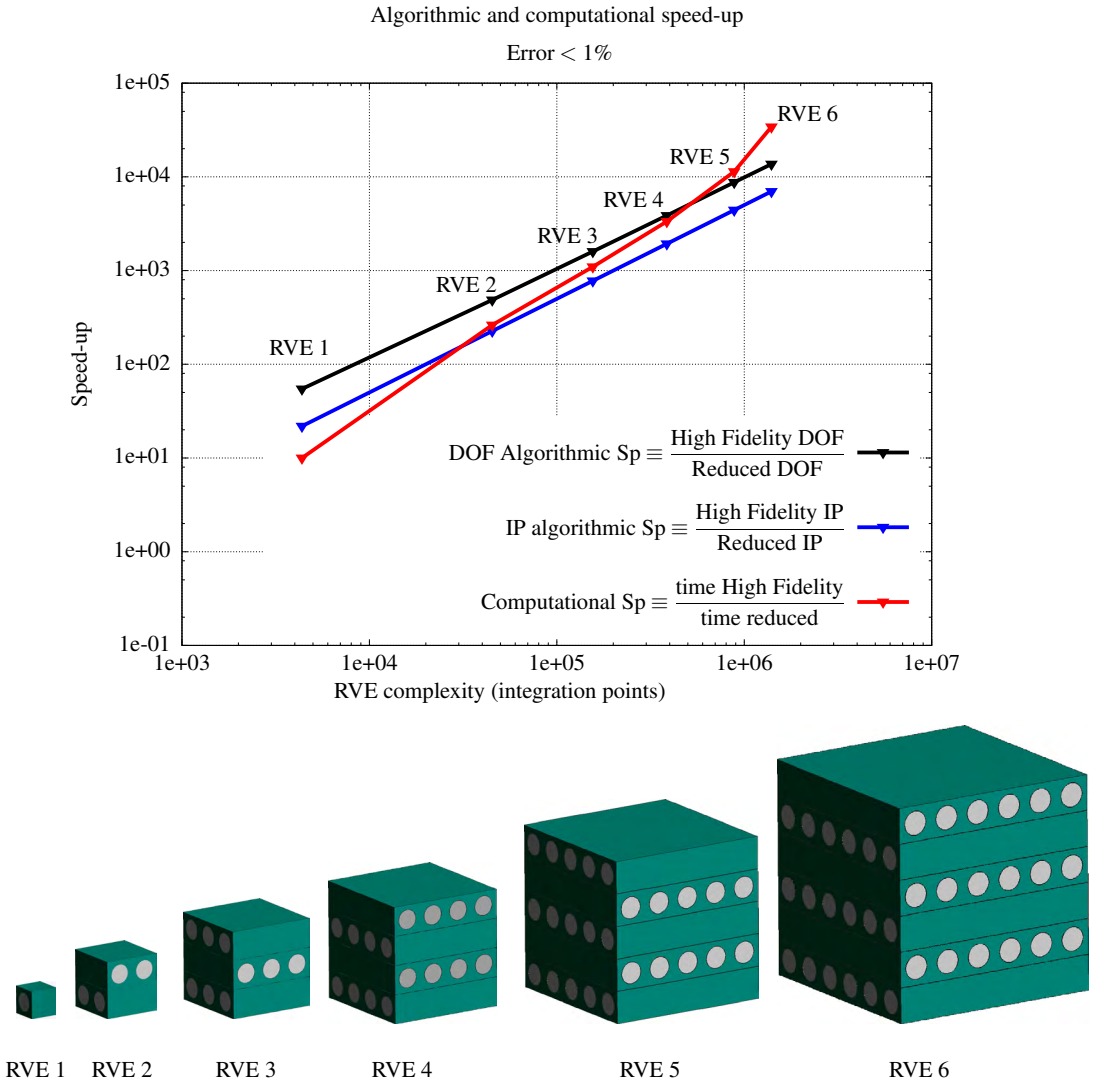

Figure 12: Speed-up values upon increasing material discretization.

3 CONCLUSIONS

The RFE^2 technology is assessed in this contribution for an industrial case study of a 3D reinforced composite laminate. A number of consistency tests have been successfully passed, i.e. convergence upon macroscopic discretization, convergence upon increasing number of reduced strain modes and convergence upon the reduced quadrature for the strain basis. Moreover, the technology proofs to be tunable upon the simulation needs of the user. In other words, different material phase parameters than the ones employed to develop the reduced bases can be adopted during the online multiscale simulation with remarkable accuracy.

The relative performance (speed-up) with respect to standard FE^2 methods increases with increasing the RVE discretization and is found between 10^4 and 10^5 for RVEs with around one million of integration points, e.g. around $100 - 150 \times 10^3$ hexahedral FE, assuming an error below 1% compared to a high fidelity analysis. These qualities are seen ideal to export the RFE^2 technology to the industrial sector.

REFERENCES

[1] Caicedo, M., Mroginski, J.L., Toro, S., Raschi, M., Huespe, A. and Oliver, J. High performance reduced order modeling techniques based on optimal energy quadrature: application to geometrically non-linear multiscale inelastic material modeling. *(2018), pp. 1–22.*

[2] Oliver J., Caicedo M., Huespe A.E., Hernndez J.A., Roubin E. Reduced order modeling strategies for computational multiscale fracture. *Comp. Meth. Appl. Mech. Eng., Vol. 313, (2017), 560–595.*

[3] Hernández J.A., Oliver J., and Huespe A.E., Caicedo, M.A. and Cante, J.C. High-performance model reduction techniques in computational multiscale homogenization. *Comp. Meth. Appl. Mech. Eng., Vol. 276, (2014), 149–189.*

[4] Feyel F. and Chaboche J.L. FE2 multiscale approach for modelling the elastovis-coplastic behaviour of long fibre SiC/Ti composite materials. *Comp. Meth. Appl. Mech. Eng., Vol. 183, (2000), 309–330.*

[5] Faria R., Oliver J. and Cervera M. On Isotropic Scalar Damage Models for the Numerical Analysis of Concrete Structures. *Technical report. Publication CIMNE N-198, (2000).*